

Modelling of cylinder system friction using P2M tool

Master's thesis in Automotive Engineering

Abhay Pandurang Pai¹, Kishan Gopal Navale²

1- Chalmers University of Technology, Göteborg

M.Sc. Automotive engineering

2- KTH Royal Institute of Technology, Stockholm

M.Sc. Engineering design – Track Combustion Engineering

MASTER'S THESIS 2016:71

Modelling of cylinder system friction using P2M tool

Master's Thesis in Automotive Engineering

Abhay Pai

Kishan Navale

Department of Applied Mechanics

Advanced Combustion Engineering Department

CHALMERS UNIVERSITY OF TECHNOLOGY

Göteborg, Sweden 2016

Modelling of cylinder system friction using P2M tool

Master's Thesis in Automotive Engineering

Abhay Pai

Kishan Navale

© Abhay Pai

Kishan Navale, 2016-08-30

Master's Thesis 2016:71

ISSN 1652-8557

Department of Applied Mechanics

Division of Advanced Combustion Engineering

Chalmers University of Technology

SE-412 96 Göteborg

Sweden

Telephone: +46 (0) 31-772 1000

Cover:

The piston from VCC used made with the help of node positions of the points.

Chalmers Reproservice

Göteborg, Sweden 2016

Modelling of cylinder system friction using P2M tool

Master's thesis in Automotive Engineering

Abhay Pandurang Pai

Kishan Gopal Navale

Department of Applied Mechanics

Chalmers University of Technology

Abstract

The internal combustion engines have been there for more than a century now and are constantly undergoing some improvements. Although the combustion engines have improved the human efficiency, it has also brought upon serious problems like the exhaust emissions. Over the last few decades, the number of automobiles have increased manifold and so has the emissions including carbon monoxide, hydrocarbons, nitrous oxides and particulate matter. This has led to global warming which has disastrous consequences if not kept in check.

The emission norms are designed to keep the automobiles emissions within a limit. These norms are becoming stringent every few years to decrease the emissions by a further extent. Car manufacturers are doing a lot of research to be ahead of the competition and be within the norm to avoid paying hefty fines. Downsizing is considered to be the future for emission reduction. The number of engines and the capacity is becoming smaller and turbochargers are installed for better power and fuel efficiency. Volvo engines for example has downsized their engines from in-line 5 cylinder to 4 and now the next generation engines are 1.5 litre 3 cylinder engines. This downsizing is one of the most effective ways to decrease the emission.

It is also known that for an engine, on an average the efficiency is only about 30 percent. Though it has increased slightly over the last few decades, it is very difficult to improve this value substantially. That is because most of the energy is lost as heat and there are friction losses in the engine. Part of the heat energy which would have wasted is used in turbochargers which have improved the efficiency. Efficiency loss due to friction is still a very big area with huge potentials and opportunities. The thesis here is divided into two parts. The first part deals with the friction calculation in the piston-cylinder system using the P2M software provided by MIT which studied the piston secondary motion to calculate the friction loss. The second part deals with the effect of changes in the inputs like the engine speed, combustion pressure etc. on the friction force and FMEP values.

Keywords: ***Efficiency, piston-cylinder system, piston secondary motion, MIT, friction force, FMEP.***

Acknowledgement

There is a long list of people who we would like to thank for the successful thesis. First and most important in list is our thesis supervisor Charbel Nassif from Volvo Car Corporation who has been our constant support and believed in our ability to take this difficult challenge and produce the best result. We would also like to thank Fredrik Strömstedt from Volvo Car Corporation who was our technical guide for the thesis and has provided valuable insight with his enormous experience in this subject and given us a good path to work on when the things became a bit complicated.

We would also like to thank our advisor from MIT Zhen Meng who has been in constant communication with us for the development of this tool to work with the Volvo inputs and helped us with his knowledge about the secondary motion of the piston. We also thank our supervisors from our universities Sven B. Andersson from Chalmers University of Technology and Anders Hulqvist from KTH Royal Institute of Technology for guiding us with the thesis work.

We also extend our thanks to our manager at Volvo Car Corporation Ingvar Åkesson and his entire team for making us feel welcome and making us a part of their team in these 6 months. We would also like to thank Lars Fahlgren from Volvo Car Corporation who offered us the opportunity to work with this thesis. We also extend our appreciation to the entire base engines team including Director Anders Agfors for the great environment that they have made for all the thesis students and especially us.

We would like to thank the CAE team of Volvo for their inputs which has been helpful for us to work with the tool.

Finally, we would like to thank our parents and our friends for their constant support during our entire time here.

Contents

Abstract.....	3
Acknowledgement	5
1. Introduction	9
1.1. Engine cylinder and piston system	9
1.2. Previous Work.....	11
1.3. Scope of the thesis work.....	12
2. Methodology.....	15
2.1. Piston Skirt Geometry	16
2.2. Compliance Matrix.....	17
2.3. Asperity Contact Model	18
2.4. Oil Transport	18
2.5. Numerical method for solution.....	20
2.6. Separation model.....	20
2.7. Calculation on grid	21
3. Results and Discussions	23
3.1. Comparison between MIT and VCC output data	25
3.1.1. Lateral Motion of the piston pin	25
3.1.2. Tilting Angle of the piston	26
3.1.3. Side force exerted by the wrist pin	27
3.1.4. Asperity contact forces	28
3.1.5. Hydrodynamic forces	29
3.1.6. Friction force	30
3.1.7. Frictional power loss	31
3.1.8. Friction energy loss	32
3.1.9. Friction Mean Effective Pressure (FMEP).....	33
3.2. Simulation Case 1: Low engine speed and low combustion pressure	34
3.3. Simulation Case 2: Higher initial oil film thickness	39
3.4. Simulation Case 3: Larger cold clearance	41
4. Conclusion.....	45
5. Future Scope	49
References	51

List of Figures

Figure 1: Piston head [3]	9
Figure 2: Piston-Cylinder Nomenclature [10]	15
Figure 3: Asperity contact piston skirt model [10].....	16
Figure 4: Mesh for piston skirt and lands [10].....	17
Figure 5: Oil supply to the system [10]	19
Figure 6: Comparison between MIT and VCC results for Lateral Motion of piston pin.....	25
Figure 7: Comparison between MIT and VCC of tilting angle of piston.....	26
Figure 8: Comparison between MIT and VCC data of side force exerted by wrist pin.....	27
Figure 9: Comparison between MIT and VCC data of asperity contact forces on thrust (left) anti-thrust side (right)	28
Figure 10: Comparison between MIT and VCC data of hydrodynamic forces on thrust (left) anti-thrust side (right).....	29
Figure 11: Comparison between MIT and VCC data of friction force.....	30
Figure 12: Comparison between MIT and VCC of frictional power loss	31
Figure 13: Comparison of MIT and VCC data of friction energy loss	32
Figure 14: Lateral motion comparison of low engine speed and low peak pressure vs. base reference case	34
Figure 15: Tilting angle comparison of low engine speed and low peak pressure vs. base reference case	35
Figure 16: Comparison of side forces between low engine speed and low pressure and the base reference case.....	36
Figure 17: Comparison of friction forces between low engine speed and low pressure and the base reference case.....	37
Figure 18: FMEP comparison between case 1 and base reference case	38
Figure 19: Comparison of results for the base case and higher oil film thickness.....	42
Figure 20: FMEP comparison between case 2 and base reference case.....	43
Figure 21: Comparison of results for the base case and higher cold clearance	42
Figure 22: FMEP comparison between case 3 and base reference case	43

1. Introduction

This chapter deals with the understanding of the engine-cylinder system and the scope of the thesis. It also includes the previous work carried out in this field over the years.

1.1. Engine cylinder and piston system

The source of power for the car is the engine. The main components of the engine which are responsible for producing the energy are the cylinder piston system. These work in conjunction with the connecting rod, crankshaft and the powertrain to transmit the energy produced in the cylinder head to the wheels. The fuel enters the cylinder head through the inlet valves and depending upon petrol or a diesel engine, the spark plug or the fuel droplets through the fuel nozzle will lead to combustion. The piston connected to the connecting rod reciprocates within the cylinder leading to rotating motion of the crankshaft which is connected to the flywheel. The transmission then transfers this power from the flywheel with the help of clutches and gears to the tires.

The reciprocating motion of the piston is called the primary motion. The expansion of the fuel which burns during the combustion process causes the piston to move in the downward direction as it is constrained in other directions due to the cylinder head. As mentioned above, this motion is responsible for transmitting the energy from the power stroke to the crankshaft. However, it is not rigidly constrained in the other directions. There is a small amount of clearance between the piston and the cylinder which is essential as the piston expands due to the heat generated in the cylinder. Although the cylinder also expands due to the heat, there is some clearance between the piston and the cylinder. This gives rise to the lateral motion and oscillatory motion of the piston which is the secondary motion. This motion is the main topic which will be dealt with in this thesis.

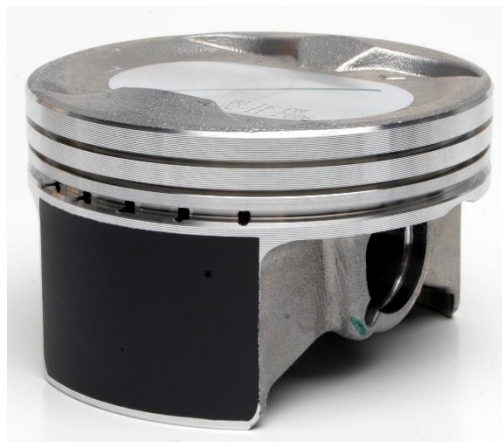


Figure 1: Piston head [3]

The primary motion of the piston accounts for only 30-35% of the total energy. Majority of the energy is wasted as heat energy and the remainder about 10% are the total frictional losses. 40-50% of this is the loss in the piston skirt-cylinder interaction. The lateral motion generates the friction between the piston and the cylinder. The tilting angle of the piston is defined as the angle with which the piston tilts towards the cylinder. The material of the cylinder liner and the material on the piston skirt as well as the oil between the piston and the cylinder play a very major role in the friction force generation within the cylinder.

The compression and the oil rings also play an important part in the friction generation. The pistons which are being used by Volvo in their engine have two compression rings and one oil control ring. The piston rings fit in the groove on the outside diameter of the piston. The main function of the compression rings is to ensure proper sealing between the top of the piston and the bottom so that no fuel or gases can pass down which might lead to further complications and loss of energy. The rings also play an important part in the heat transfer to the cylinder wall as they are in direct contact with it. Finally, the oil ring regulates the oil consumption during the strokes [2]. These areas with the rings are referred to as lands. The top of the piston along with the first compression ring is the top land followed by the second and the third land. There exists a chamfer region between the third land and the piston skirt. The piston skirt is the part of the piston which controls excessive rocking of the piston. It also has total contact with the cylinder wall and is the most important part to focus on while studying the lateral motion of the piston.

The oil thickness in the regions mentioned above especially between the piston skirt and the cylinder and in the chamfer region has a significant impact on the hydrodynamic forces generated by the piston. Thickness of the film is usually in the range of about 20-40 micrometres. The oil is splashed in to the piston from the oil sump and then flowing in the area between the piston skirt and the cylinder liner. The oil scrapes through the cylinder liner with the help of the piston rings before returning to the oil sump. The chamfer region acts as an oil reservoir.

The material of the cylinder liner and the piston skirt are important factors to be considered for friction. The cylinder liner material is different than the material of the cylinders as its functions are different. The main reason for this is that the cylinder liner has to resist corrosion and also be wear resistance at high temperatures. It also protects the piston surface and the piston rings from wear damage. But it is necessary for the liner material to withstand the high pressures, vibrations etc. along with the high temperatures. A few possible options for the cylinder liner material are carbon steel, cast PH stainless steel, cast nickel-chromium alloy, low alloy steel, and wrought PH stainless steel [4]. A research carried out by M.F. Fakaruddin et al. [4] found out that based on durability,

operation requirements in extreme temperatures and wear resistance properties, the cast nickel-chromium alloy or more commonly known as Inconel 713C was the best material for wet cylinder liner applications.

Volvo uses grey cast iron as the cylinder liner material for the cylinder block which is made from aluminium. Grey cast iron has good wear resistance, good vibration damping among other properties like corrosion resistance and being able to withstand higher loads. These properties make it one of the most efficient cylinder liner materials.

The piston skirt on the other hand is usually coated with a different material. The piston these days are mostly made from aluminium or aluminium based alloys for its light weight advantages. The piston skirt is coated with graphite. The main advantages for using graphite are that the material is very well known for low friction and is more durable than other coatings. This makes it ideal to be used in car pistons as this leads to lesser wear and lesser repair and maintenance costs. Other materials for the piston skirt include polymers, composite coating with resin binder with fillers [5].

The friction generated between the piston-ring assembly and the cylinder liner accounts for about 50 % of the total engine mechanical loss as stated by Tian Tian [6]. He states that in order to reduce the friction coefficient, there exists an optimum level of oil viscosity above which the boundary lubrication might introduce friction. A lot of work has been done over the last two decades in the field of reducing the friction generated in the cylinders. Some of the important work related to the thesis will be discussed further.

1.2. Previous Work

The reduction of engine friction is an important research for improving the efficiency of the engine. Reducing friction will not only save more fuel as lesser fuel will be required to produce the same energy but also improve the life of the cylinder liner and the piston material as lesser forces would mean lesser scraping of the material. This would lead to lesser repair and maintenance thus making the vehicle more desirable to the customers.

Massachusetts Institute of Technology (MIT) has done huge amount of research work in the field of friction in the cylinder-piston system. Volvo Car Corporation is in collaboration with MIT developing a software tool called P2M (piston secondary motion) which can be used to find out the friction force and the tilting angle of piston as well as the FMEP and the friction coefficient values. Getting accurate results from this tool is important as these can then be used and the piston skirt modified or oil consumption levels changed to get lesser friction forces. MIT has been trying to improve this

tool for over a decade now and many thesis works have been carried out with the help of previous versions of this tool. A few relevant thesis topics will be discussed further.

Most of the work focussed on using the P2M tool and the Laser Induced Fluorescence (LIF) visualization system to understand the simulation process and to visualise actual real time results and then compare the two results. Benoist Thirouard [7] carried out research in modelling oil transport in piston ring pack by implementing two dimensional LIF system and presented an oil transport scheme by integrating the major paths and mechanisms of oil transport in the piston. Camille Baelden [8] quantified the impact of deformation of the cylinder with thermal expansion, tilting of the piston and the oil collection in the chamfer region on the oil flow between the piston and the cylinder. These research works were vital for the development of the P2M tool as it takes into account the results from all these topics to give a realistic value of the frictional force and the oil flow. An initial oil film thickness is also defined in the input model for the tool to work and this is achieved by studies conducted by Benoist and others mentioned above.

One of the most important works carried out in the P2M development field is the research by Conor McNally [9] who in the year 2000 made numerical model calculating the piston secondary motion which can then be used to simulate on the computer by writing a code. The piston assembly is considered to be a set of independent rigid bodies and equations of motions are formulated for each part. Reynolds equation is computed for the oil film to achieve the hydrodynamic force. This is carried out at several circumferential points (nodes) of the piston and the integration of all these give the total lateral force generated by the piston on the cylinder. This is the heart of the P2M tool. Future research has been carried out on this to include various additional scenarios like cylinder deformation and deformation due to pressure and inertia in the piston to obtain close to real test rig values for the FMEP.

1.3. Scope of the thesis work

The cylinder system stands for a major part of engine friction, both with loaded and motored engine. For tougher friction target and increased engine specific loading, all other targets and requirements for the engine still needs to be fulfilled mainly NVH, oil consumption and durability. Cylinder deactivation on petrol engines can reduce CO₂ due to better brake specific fuel consumption on non-deactivated cylinder; however, it is affecting the oil consumption drastically.

Working with simulation tools is essential to be able to optimize the system. Volvo Cars has unique capabilities for simulating cylinder system friction and correlate simulations with measurements. On the simulation side, Volvo Cars is working in close cooperation with MIT – Massachusetts Institute of

Technology who is developing simulation tools for lubrication in internal combustion engines. The goal of the thesis is to work on the oil transport and the friction in the piston cylinder assembly. P2M tool from MIT is used to calculate the oil transport and friction for different cases while running the engine. The main objective is to tune the data generated by the FEA team at Volvo Car Corporation in a format which can be used for the tool. The results including the lateral motion, tilting angle, friction forces among others has to be obtained by running successful simulations for the Volvo piston.

2. Methodology

Before understanding how the research and simulation for the thesis was carried it is very important to be familiar with the definitions that will be used in this report often.

Consider the base engine as shown in the figure 2. The two dimensional view shows the aspects of the piston and the cylinder. The main input for the tool is the definition of the thrust and the anti-thrust side of the piston. The left side of the cylinder is the thrust side and the right is the anti-thrust side. In three-dimensional sense, the surfaces of the piston from the midpoint to the left end are considered to be lying on the thrust side and so on. The naming in the above figure will be explained in detail in the Input Manual.

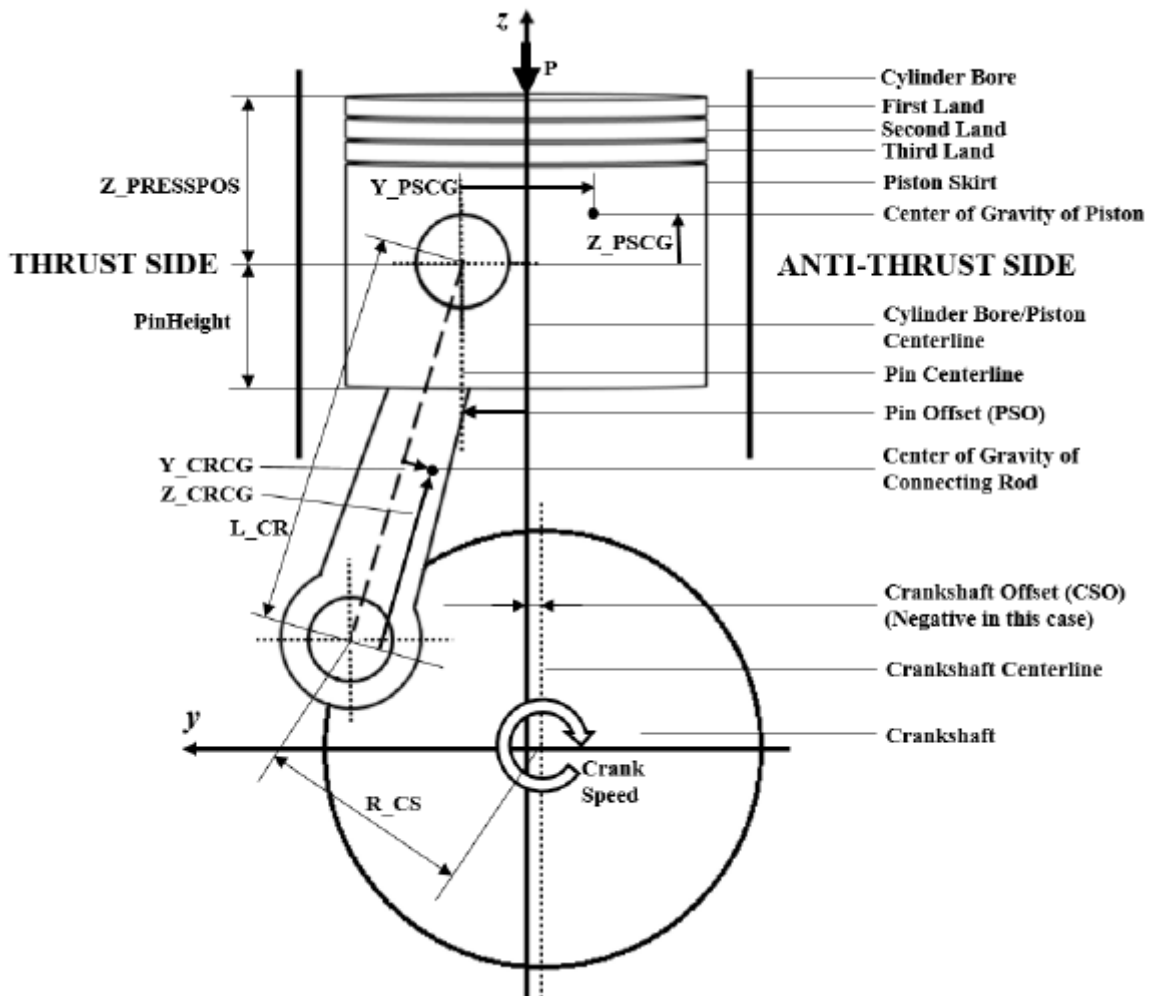


Figure 2: Piston-Cylinder Nomenclature [10]

In order to simplify the calculations which the tool takes into account for generating the outputs, there are certain assumptions which are made [1]:

- Connecting rod big end is frictionless and can rotate freely relative to each other.
- Wrist pin bearing is frictionless. This simplifies the calculations immensely. If the friction for this part is considered, it would lead to creation of more mathematical models which takes into account the lubrication of the bearing.
- Engine speed is assumed to be constant throughout the whole cycle.
- Wrist pin centre of gravity is assumed to be at the centre of the piston pin hole on the z-axis as the pin offset Y_PSCG is considered 0 in the simulations run for this thesis.

The complete dynamics and kinematics based along with the relevant equations on which the tool has been developed has been explained in the thesis ‘Modelling Piston Skirt Lubrication in Internal Combustion Engines’ by Dongfang Bai [1] from MIT. In this thesis, the main parts of it will be elaborated which has relevance to the topics being dealt for the current research.

2.1. Piston Skirt Geometry

The piston skirt has ovality along the circumference. The thrust and anti-thrust have been defined earlier and the pin axis is perpendicular to the two sides. The piston has more diameter along the piston skirt to prevent the top lands brushing against the bore and the friction is only focused in the skirt area. The surface roughness and wavelength of the piston skirt is also defined in the input model. To give a better understanding of the same, refer figure 3.

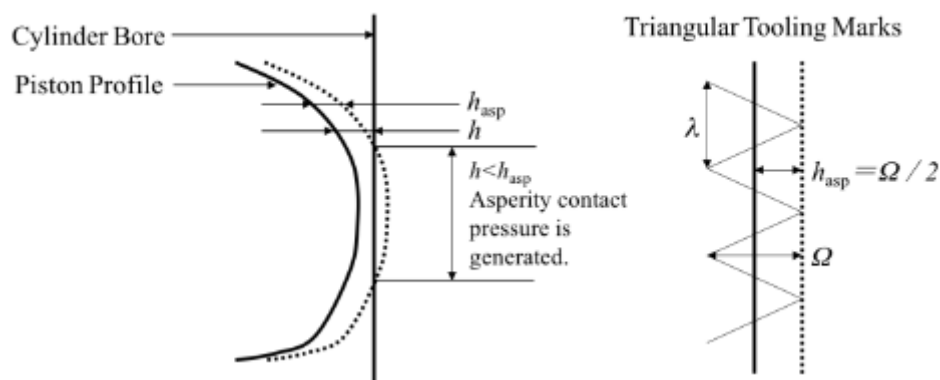


Figure 3: Asperity contact piston skirt model [10]

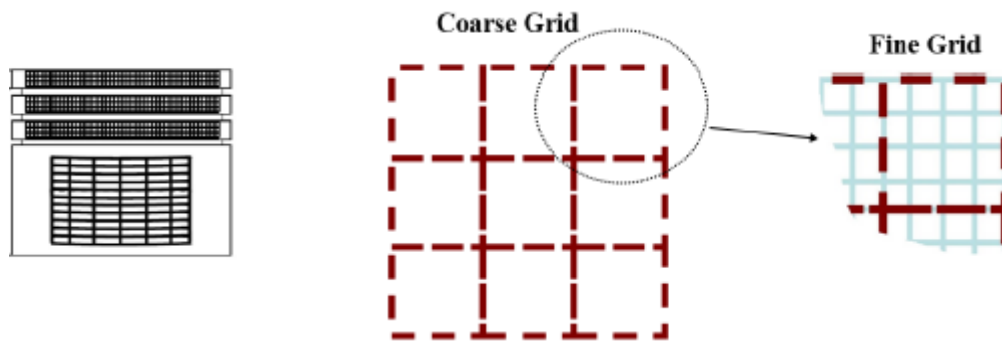


Figure 4: Mesh for piston skirt and lands [10].

The piston skirt is the main area of interest for the tool. By defining the piston skirt area, the calculation domain is generated. The tool will then work in the calculation domain taking into account the piston skirt and the piston top land for generating the result. As stated in the literature above, the tool applies numerical method of calculation for the piston. This is done by generating grids or meshes and the points at the intersection are the node points at which the forces and the various parameters are calculated. The reason for the coarse grids and the fine grids for specific calculations has been described in the further part of the methodology. These mesh points are mainly used for generating all the output parameters. For getting a general idea about the grid mesh, refer to the figure 4.

2.2. Compliance Matrix

The skirt and the liner are considered to be flexible bodies by the tool so they undergo deformation when loads act on it. These deformations are due to the combustion pressure and engine speed which give rise to force due to pressure and inertia forces. These two inputs are defined in the input files by the user as well.

The piston skirt is divided into coarse and fine grids as shown above in figure 4. The deformation of the nodes d is vector as it is defined in the x , y and z directions. The force which acts on the nodes is F . Compliance C is a constant which relates the deformation to the force as

$$d=C*F$$

The piston pin is locked and the deformation at each node is calculated with unit force. This is then saved in a matrix form which satisfies the compliance equation mentioned earlier. In the current analysis, the compliance for the Volvo piston skirt was available and is used and a definite necessity for the tool to process the input and move towards the next step which is running the main P2M tool. The one for the liner was not calculated but the tool can take the liner compliance into account and give better results.

2.3. Asperity Contact Model

When the piston skirt has contact with the bore, there will be surface to surface contact along with the hydrodynamic lubrication. This contact is defined as the asperity contact. It is necessary to calculate the pressure generation due to this asperity contact. The asperity depends on the surface geometry and the material used. The wavelength Λ and the wave height Ω is defined in the input model. Also refer figure 3 for visual understanding of the surface roughness and tooling marks. Analytical solution is used for a blunt wedge against a plane to calculate the asperity contact pressure [10] given as

$$P_{asp} = \begin{cases} C_1 \cdot (h_{asp} - h)^{c_2}, & h > h_{asp} \\ 0, & h \leq h_{asp} \end{cases}$$

Where h is the height of the tool marks and can also be seen from figure 3.

The program will calculate the constants C_1 when the other inputs like wavelength, wave height and the Young's Modulus is specifies in the input model file.

2.4. Oil Transport

The oil thickness within the piston and the cylinder plays a vital role and is governed by the boundary condition defined for it. The system is divided into three parts namely the chamfer area just below the oil control ring, the skirt region and the oil on the liner below the skirt. The clearance between the chamfer and the liner is much bigger compared to the skirt and holds more oil and also acts as oil reservoir which feeds oil in the skirt region during the motion of the piston. The oil exchange with the surroundings includes oil splash to the liner, scraping down of oil when the piston moves down towards the bottom dead centre position and oil released through the oil control ring grooves or drain holes. The initial oil film thickness and the oil splash are defined in the input model. The current simulations for this thesis do not consider additional oil supply to the system as the input file for the same is not defined. When the skirt and the liner are in direct contact with each other, no oil can pass due to zero clearance. This statement is true when a perfect straight shape is assumed for the liner and the triangular tooling marks are assumed for the skirt. In reality however, the shapes are not perfect and there will always be a thin film of oil that can pass through these irregularities. The oil film thickness in solid to solid contact in the tool plays importance as too small value will lead to rapidly changing pressure profiles which cannot be captured on the fine grid. In the input, an initial value is set and the program automatically increases the oil film thickness when convergence is hard to achieve. The flow phenomena governing the oil motion is the Couette and Poiseuille flow where the oil attachment occurs between the piston skirt and the cylinder liner.

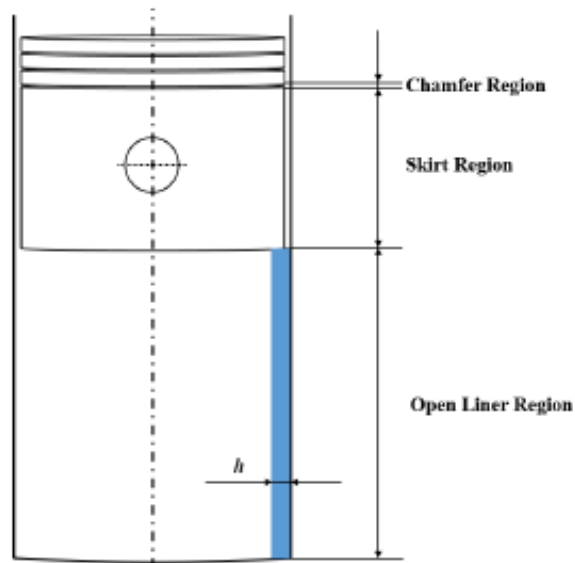


Figure 5: Oil supply to the system [10]

The details of the oil flow during the piston motion is explained in detail in Dongfang Bai's thesis [1] and a summary of that study has been presented in this thesis report.

The equation which is used to solve the oil in the skirt region is the Universal Reynolds' Equation with separation. The thickness of oil within different regions of piston mentioned earlier and the liner changes as the piston moves from top end to bottom end and vice-versa. This is because of the inertia of the piston as well as the scraping of oil and such other factors. This leads to different boundary conditions for the calculation of the oil film by the tool at different piston positions.

When the piston is moving downward, till mid-position, the inertia will be acting upwards which pushes the oil in the chamfer region upwards while when the piston moves from the mid-stroke to downward position, the inertia acts downwards and will move the oil downward relative to the piston. At this instant, the oil may move from chamfer to the skirt region. But as the liner is moving up relative to the piston, it tries to push the oil back in the chamfer region leading to oil recirculation in the chamfer region.

When the piston is moving upwards after the bottom dead position, the inertia first acts downwards till the mid-stroke position and will push oil downwards relative to the piston. Also the liner moves downward relative to the piston which also pushes the oil downwards. After mid-stroke however, there is less oil in the chamfer region as lot of oil from the chamfer seeped to the skirt region. Piston deceleration and the inertia acting upwards forces the oil to move upwards relative to the skirt back into the chamfer area.

One of the features of the tool is that the calculation for the hydrodynamic and asperity contact is done in the skirt region only and this is fine as this phenomenon occur only in the skirt region and not in the chamfer or the land region to a great extent.

2.5. Numerical method for solution

The universal Reynolds' equation is used to solve the hydrodynamic forces and asperity forces while considering the motion of the oil in the piston-cylinder system. The piston skirt area is divided in grids as shown in Figure 4. For complete method of defining the variables and solving the Reynolds' equation refer to chapter 4 of Donfang Bai's thesis report [1]. The mass flow of the oil during the upward and downward motion of the piston is calculated with the equations for mass flow written for each case, the details of which are available in the mentioned chapter above.

Some assumptions for the Reynolds' equation that the tool uses are described below [12]:

- The oil is Newtonian for the equation to be true.
- The fluid viscous forces are much higher in magnitude than the inertia forces which is the main principle of the Reynolds number.
- Variation of the oil film is negligible.
- The oil film thickness is much less than the width and length of the surface which negates the effect of curvature.

2.6. Separation model

The solution using Reynolds' equation assumes full attachment assumption in the partial film region and does not consider separation phenomenon. There is a different separation model defined for the tool as separation occurs at different phases within the piston-cylinder system. Two control volumes are defined with one which has oil on the piston skirt and the other similarly on the liner. These oil films are separated. The local oil fraction is calculated for different phenomenon which assumes either full attachment or separation. This local oil friction is the average of the oil film thickness on skirt and the liner surface respectively.

If ho_s is the oil film thickness on skirt surface and ho_L is the oil film thickness on the liner surface and h_c is the local clearance between the two surfaces.

The local oil fraction is given as follows

$$\text{Local oil fraction} = \frac{ho_s + ho_L}{h_c}$$

Total separation occurs when there is gas between the oil film of the skirt and the liner. A threshold is defined in the model and the oil fraction less than this value implies separation or else full attachment. To solve the model, the Couette flow term which consists of the product of the local oil fraction, displacement in x-direction (secondary motion direction) and magnitude of z-direction displacement (reciprocating motion direction) and the time step with the oil film thickness on liner is calculated using explicit method before each time step. This means that the oil fraction of the control volume as defined earlier at previous time is checked. Finally, a set of equations are formulated which have been explained in Bai's research paper [1] based on which the tool computes the different outputs discussed in the results section of the report.

One drawback of this method is that the tool takes time steps meaning jumps when it changes from partial film to full attachment as it crosses the threshold number. In reality, the transition is smoother and so the calculation is not 100 percent accurate but is necessary to be able to form equations for solving the partial film phenomenon.

2.7. Calculation on grid

The structural deformation is defined on the coarse grid as the deformation is generally smooth and using a coarse grid will not lead to a significant loss of accuracy. The lubrication calculation on the other hand needs to be very accurate as the pressure distribution depends on the oil availability and is hence defined on the fine grid. Interpolation over the coarse grid is used to define the deformation over the fine grid. Lubrication calculation, pressure distribution, oil transport and the shear stress is calculated on the fine grid while the normal forces and frictional forces is calculated on the coarse grid first and the results are then interpolated to get the final output over the fine grid.

The crux of the tool is to define the input in the way that the tool requires. The piston, bore are defined by their node positions. Thermal deformations of those are taken into account and are defined by node positions. The deformation due to inertia of the piston and the combustion pressure is also defined by the node positions of the deformations. Thus, it is necessary to define the node positions properly to be able to get accurate results. This thesis work dealt mainly with correcting the input data generated by the FEA team as the data format was not compatible with the requirement of the tool.

3. Results and Discussions

The main output from the P2M tool are lateral motion of the piston pin, tilting angle of the piston, the normal forces exerted on the piston, the hydrodynamic forces due to the oil film, the friction forces and the friction mean effective pressure. The plots from the MIT piston were used as a reference to understand the similarities and the differences with the VCC piston. The description of the above mentioned parameters are as follows

- Lateral Motion – The piston motion during the cycle is seen with the help of a plot. The piston pin motion at different crank angle degrees is plotted. The motions towards the anti-thrust side are represented as negative values while the motions towards the thrust side are represented as positive values. The lateral motion depends on factors like the clearance between the cold piston and bore, the thermal expansion of the two once the cycle starts and the oil film thickness between the different parts of the piston namely skirt, chamfer area and the lands and the bore.
- Tilting Angle – The piston has the tendency to tilt because of the clearance that exists between the piston and the bore. This tilting in degrees is the second output plotted. It gives an idea about which direction the piston tilts and by how much at different crank angle degrees. Positive values here indicate that the piston tilts clockwise and negative values indicate anticlockwise direction. In other words, positive values mean tilting towards the anti-thrust side and the negative values means tilting towards the thrust side of the cylinder.
- Normal forces exerted on the piston – This plot gives the magnitude and direction of the asperity contact force, hydrodynamic force as well as the side force exerted by the wrist pin on the piston. Positive values for the side force indicate the force is pointing to the thrust side and negative values to anti-thrust side. The asperity contact forces are significant in understanding the magnitude of forces when the piston hits the thrust or the anti-thrust side at different angles. It gives a good idea about the motion of the piston at different crank angles helping understand what happens during the reciprocating motion of the piston at different strokes.
The hydrodynamic force results from the oil film in the clearance between the piston and the cylinder. This layer of oil film keeps changing because of the thermal expansion as well as reciprocating motion of the piston. This oil film is very important to decrease the friction as it lubricates the area between the piston and the cylinder. Without this layer, the asperity contact force as well as the frictional forces would become very high.
- Frictional force and frictional losses – The friction force resulting due to the secondary motion of the piston is plotted for every crank angle degrees over a cycle. The power loss and energy loss

due to the friction force is also plotted on the same graph. The power loss is then used to calculate the Friction Mean Effective Pressure (FMEP).

- FMEP – The FMEP value is saved in a text file for the whole cycle. There are 5 columns which indicate the FMEP over the cycle, FMEP on thrust and anti-thrust and FMEP from asperity contact on thrust and anti-thrust side respectively. For the tool to generate FMEP values, it needs to run at least for 1 cycle or 720 degrees.

A number of different simulation cases have been run to understand the consequences of changing different input parameters like pressure, cold radial clearance, oil film thickness etc. on the friction force and other outputs as mentioned above.

MIT case has been taken as a reference to compare with the VCC piston results. The following plots show the difference in various parameters as described above of these two cases. The plots below show the curves over 2 cycles of a 4-stroke engine i.e., 1440 crank angle degrees. This is done to see the repeatability of the results after the first cycle. An explanation for the differences between the two pistons will follow in the coming explanations.

3.1. Comparison between MIT and VCC output data

3.1.1. Lateral Motion of the piston pin

The lateral motion of the piston pin depends largely on the available clearance between the piston and the bore. The final value takes into consideration the thermal deformations of the bore and the piston skirt and the surface roughness along with the nominal diameter of the bore and cold which is specified in the input model file.

The positive values indicate the motion of the piston towards the thrust side and the negative values indicate the motion of the piston towards the anti-thrust side. The lateral motion of the MIT piston ranges between 30 micrometre on thrust side and 15 micrometre on anti-thrust side. In case of the Volvo piston the variation is between 15 micrometre on thrust side and 9 micrometre on anti-thrust side. This is attributed to the fact that the clearance between the final positions of the piston skirt and the bore is higher in case of MIT than in case of VCC. It can also be seen that the lateral motion is maximum just after the combustion thus proving that the maximum lateral motion occurs immediately after the power stroke.

It can be observed that the lateral motion is same at a few crank angle degrees. This is due to few errors in the input files that were available. With appropriate input files, the curve would be similar to the MIT piston.

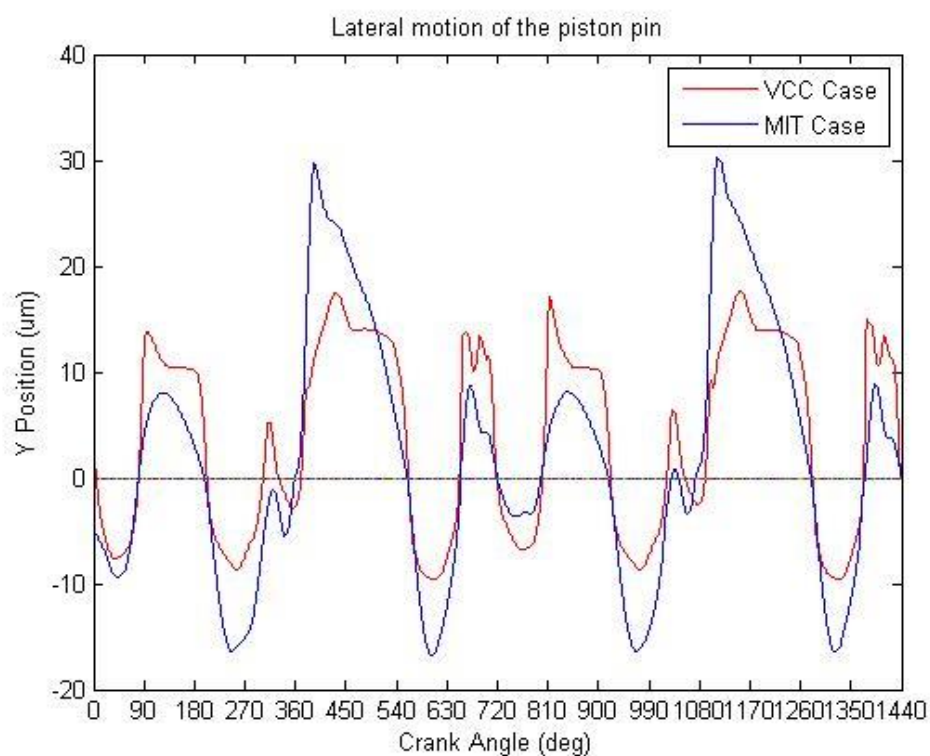


Figure 6: Comparison between MIT and VCC results for Lateral Motion of piston pin

3.1.2. Tilting Angle of the piston

Figure 7 shows a lot of deviation between the MIT piston and the VCC piston. Positive values indicate the tilting of the piston clockwise and the negative values indicate the tilting of the piston anti-clockwise. The MIT piston data shows the tilting angle variation between 0.24 degrees clockwise to 0.12 degrees anti-clockwise. The VCC data shows the same between 0.12 degrees approximately on both sides. This is as a result of lesser clearance as well as no piston pin offset. The pin offset is defined in the input model. For VCC simulations the offset was 0 in this simulation case while MIT had a pin offset of 0.5 mm.

It can also be observed that the curve followed by both the curves varies quite a bit. While the MIT tilts on one side for more crank angle degrees, the VCC piston turns the other way every time the stroke of the piston changes from top to bottom and vice-versa. The maximum tilting angle is during the intake stroke as against the power stroke seen in case of MIT. The reasons for these anomalies range from input data to the compliance matrix data available from the FEA department which was calculated for steel piston instead of aluminium. However, it is not possible to pin point on these reasons for the deviations seen in figure 7.

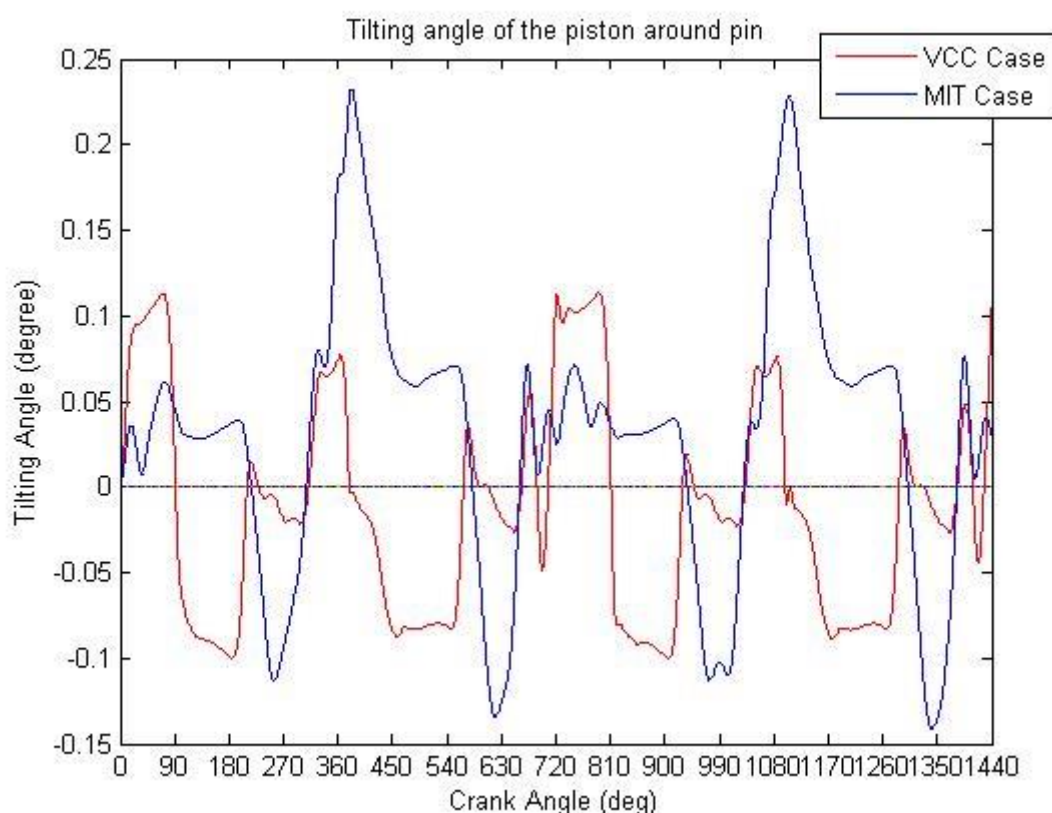


Figure 7: Comparison between MIT and VCC of tilting angle of piston

3.1.3. Side force exerted by the wrist pin

Figure 8 shows the side force exerted by the wrist pin to the piston skirt. The positive values indicate the magnitude of the force on the thrust side and the negative values indicate the magnitude of the force on the anti-thrust side. As seen above the Volvo data and the MIT data are almost identical in the curve path followed. This shows that as far as this data is concerned, it depends mostly on the crank-pin data specified in the input model and the input pressure apart from the clearance. It does not depend on other input data needed for various other parameters which might have given rise to anomalies if it did.

The maximum force is just after the spark ignition in the engine. This makes sense as the extreme pressure after the ignition will result in maximum side forces. The magnitude of the side force is higher in VCC than in MIT case. This is because it depends on data defined in the input model which includes pin offset, moment of inertia of the piston, connecting rod and the pin, and the weight of the piston as well.

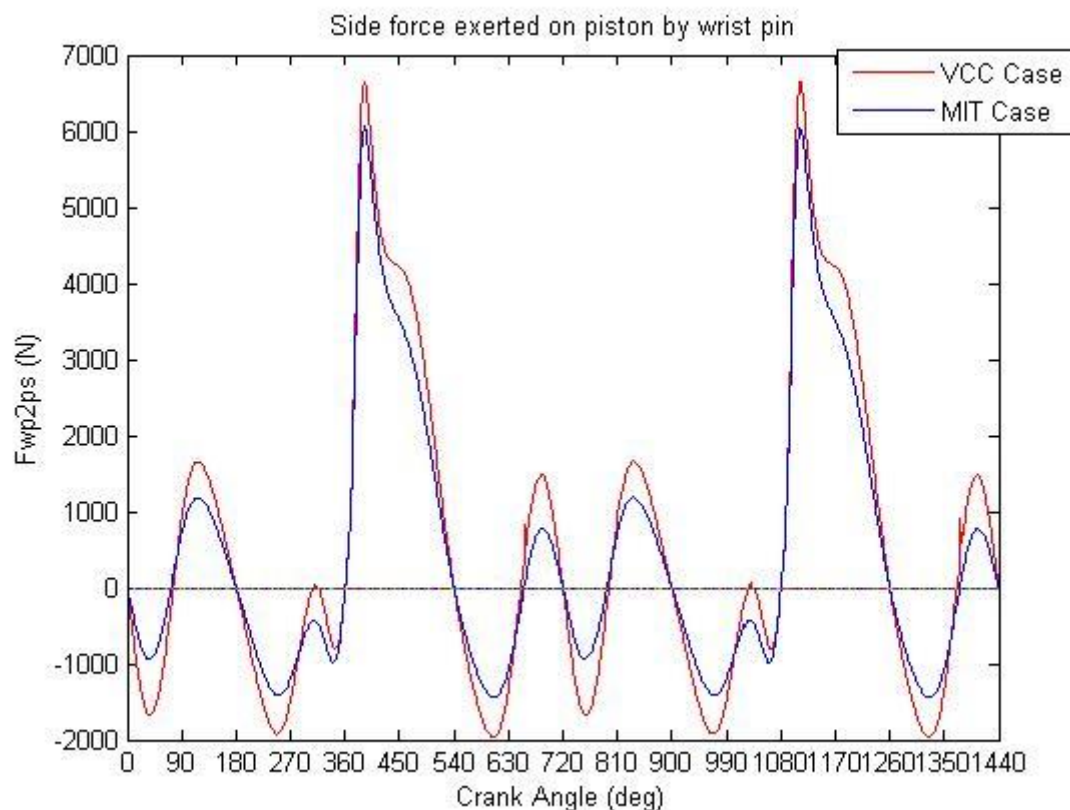


Figure 8: Comparison between MIT and VCC data of side force exerted by wrist pin

3.1.4. Asperity contact forces

Asperity is defined as the surface unevenness or the roughness of the material. The force due to the roughness on the thrust and the anti-thrust side called the asperity contact forces are shown in figure 9. The magnitude of forces are much higher for the VCC piston compared to MIT piston on the thrust side while the anti-thrust side, the MIT does not have asperity contact after the initial 20 crank angle degrees.

The higher forces on the thrust side show that the piston hits the thrust side more than the anti-thrust side during the cycle. This is also corroborated by the lateral motion plot where the lateral motion towards the thrust side is higher than the anti-thrust side. The peak for the asperity force occurs after ignition towards the anti-thrust side which has a magnitude of 5000 N approximately. This shows that the piston is moving towards the thrust side after the ignition.

The anti-thrust side for the VCC data in comparison to the MIT data shows a lot of variation. There is an anti-thrust asperity contact force up to a peak of 630 N for VCC piston. The asperity contact data depends on the surface roughness of the material as well as the clearance between the piston skirt and the bore. This might be one of the reasons for the difference in the results.

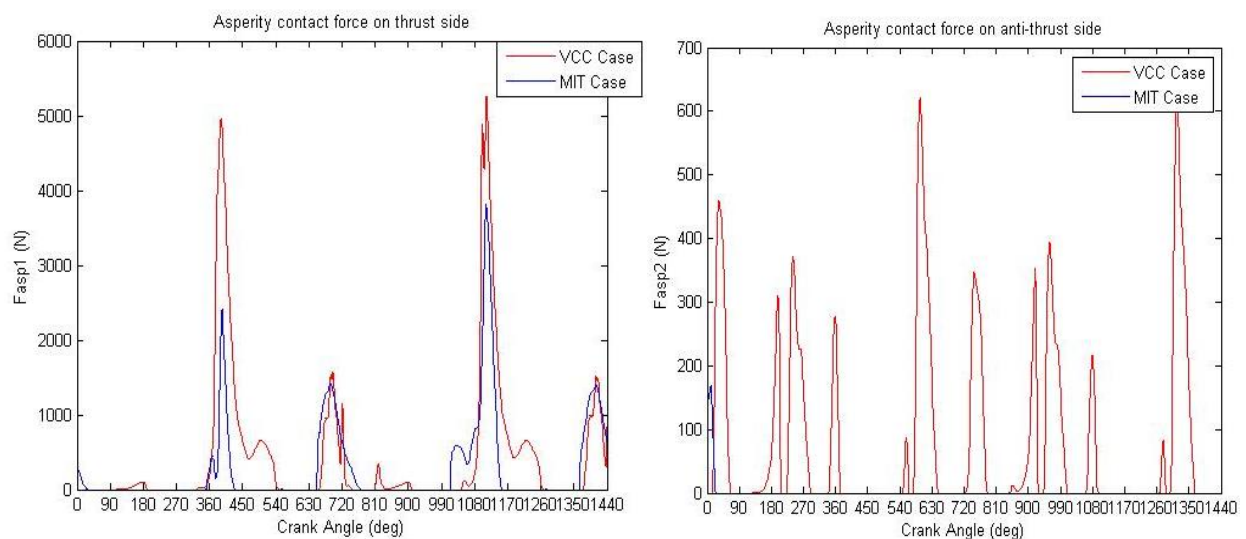


Figure 9: Comparison between MIT and VCC data of asperity contact forces on thrust (left) anti-thrust side (right)

3.1.5. Hydrodynamic forces

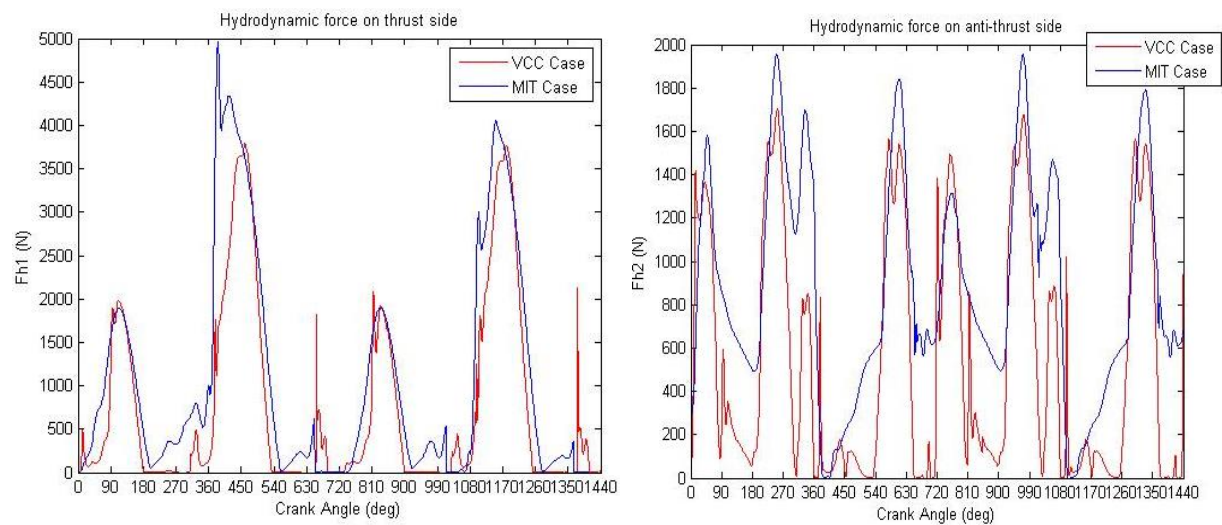


Figure 10: Comparison between MIT and VCC data of hydrodynamic forces on thrust (left) anti-thrust side (right)

The forces exerted on the oil film thickness due to the lateral motion of the piston skirt towards the thrust and the anti-thrust side are the hydrodynamic forces shown in figure 10. The peak forces are maximum after ignition on the thrust side and as seen the MIT has higher hydrodynamic force on both thrust and the anti-thrust side.

The hydrodynamic forces exerted by the piston skirt on the liner have a lot of significance on the friction forces. With proper lubrication, the effects of piston scuffing can be reduced by a great extent. In the simulation cases, only the initial oil film had been defined in the input model and additional oil film supply during the piston motion has not been considered. With the addition of that file, the results for the hydrodynamic forces and the resulting friction would vary compared to the base reference cases which have been evaluated in this thesis work.

3.1.6. Friction force

The data generated in this column through the tool is the most important output for this thesis. It gives the forces due to the secondary motion of the piston at the skirt-liner interface. The positive values indicate the friction forces on the thrust side and the negative values indicate the forces on the anti-thrust side. As seen in figure 11, the nature of the curve in both the cases is the same. The friction force is towards the thrust side when the lateral motion is towards the thrust side and vice-versa.

The magnitude of forces in case of Volvo piston is higher than that of MIT piston. The peak value of the MIT data after the ignition is 137 N in the second cycle while for the peak value for the VCC data at the same crank angle is 183 N. The friction force depends on the friction coefficient of the surfaces in contact which was higher in case of VCC at 0.08 as opposed to MIT which was 0.03. It also depends on the oil film thickness the final clearance between the piston skirt and the bore after the thermal expansion.

Also, the VCC friction data is slightly erratic compared to the MIT data. The reasons for this are similar to the difference in results in previous cases like error in compliance data and inertia and pressure deformations. Bore thermal deformations used are MIT's as the VCC data was incompatible to be used with this tool.

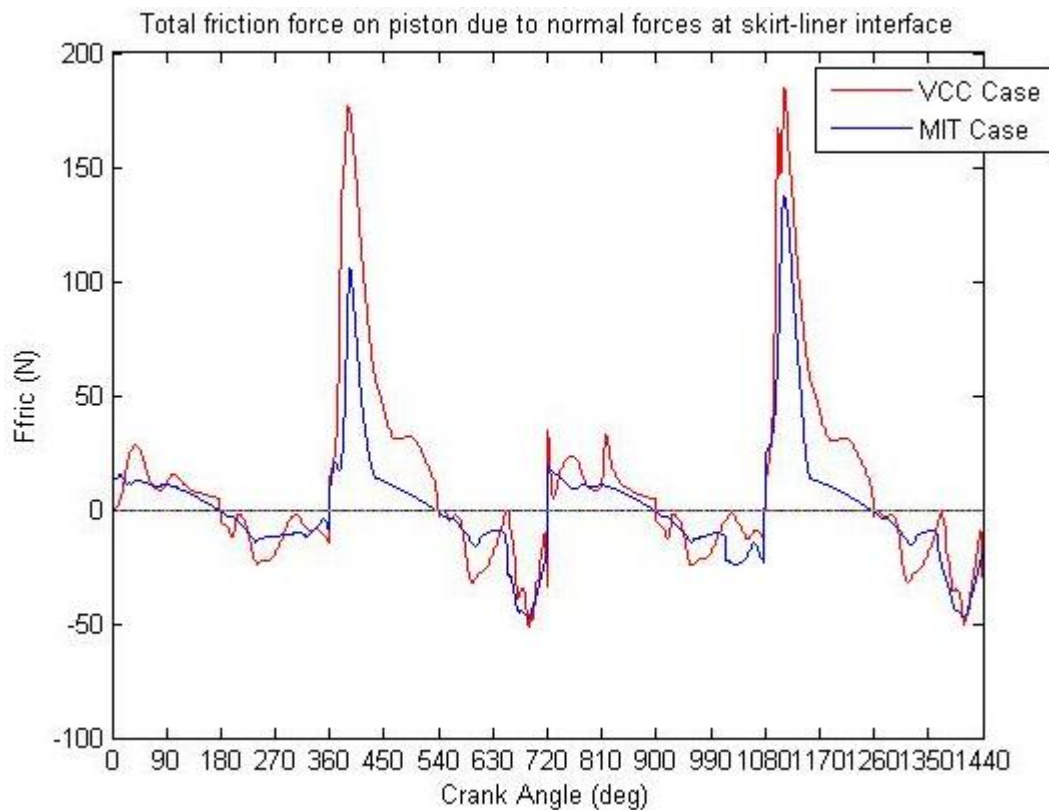


Figure 11: Comparison between MIT and VCC data of friction force

3.1.7. Frictional power loss

The power loss due to friction data is used for calculating the FMEP values over the complete cycle. The trend that the two pistons follows is similar as seen in the plot above but the peak values of the VCC piston are higher approximately 3460 W compared to 2340 W of the MIT piston. This power loss is the power lost to overcome the friction between the piston-cylinder systems. In other words, this graph must follow the same pattern as the friction forces plot in the plot above. The power loss data is available only in terms of magnitude and not in direction hence no thrust and anti-thrust power loss separately. However, the power loss and the friction plots can be compared to understand when the power loss happens towards thrust and anti-thrust.

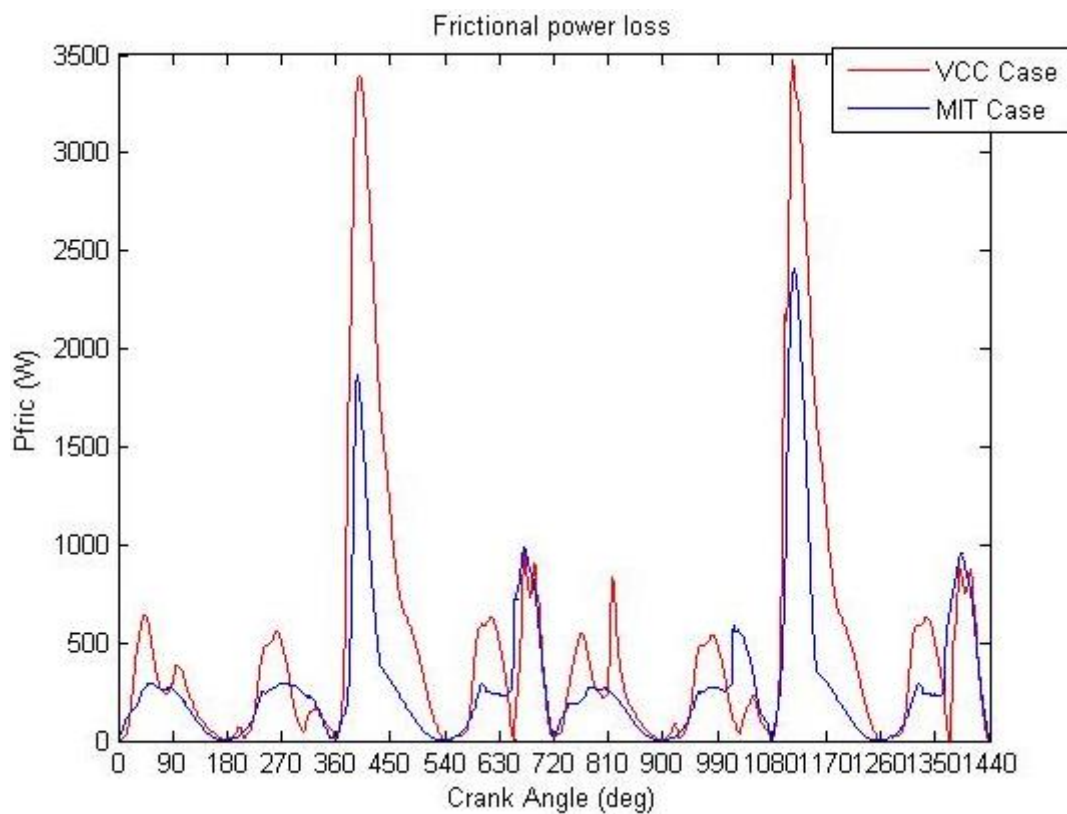


Figure 12: Comparison between MIT and VCC of frictional power loss

The FMEP is calculated from the power loss by the following formula:

$$FMEP = \frac{P * N * 600 * n_c}{V_d * n}$$

FMEP = Friction Mean Effective Pressure over the cycle (bar)

P= Frictional Power Loss (Watt)

n_c = Number of revolutions per cycle which is 2 for a 4-stroke engine

V_d = Displacement volume (cu.m)

N= Engine Speed (rpm)

3.1.8. Friction energy loss

The final plot output from the tool is the work friction energy loss. The curve trend is similar in both cases and the peak values are 11 J for Volvo piston and 7 J for MIT piston. The maximum energy loss as seen in figure 12 is at the end of each cycle as it is not the absolute value but the accumulated friction energy loss over the complete cycle.

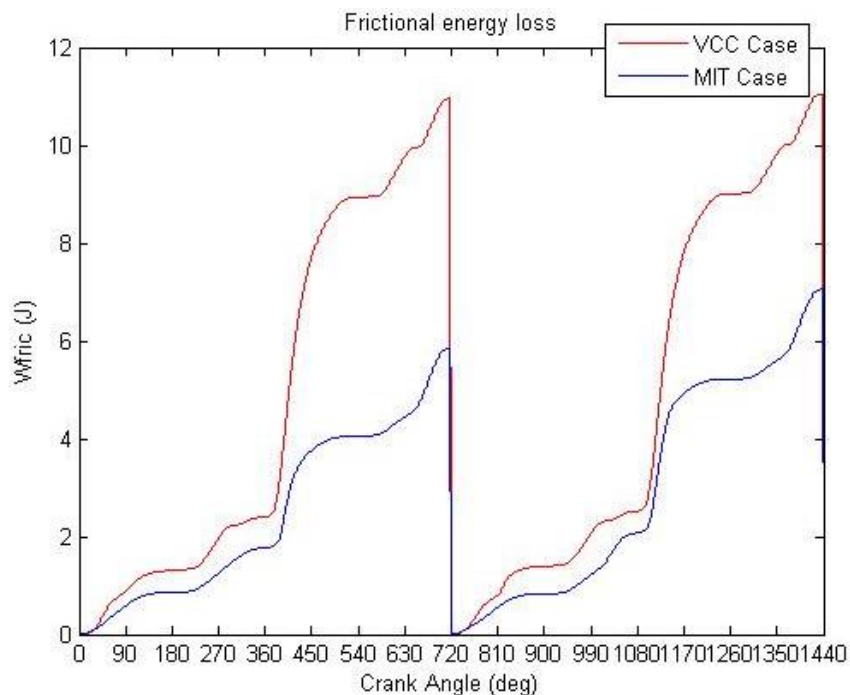


Figure 13: Comparison of MIT and VCC data of friction energy loss

3.1.9. Friction Mean Effective Pressure (FMEP)

Table 1: Comparison of MIT and VCC of FMEP values (all values in bars)

MIT	FMEP (i^{th} cycle)	FMEP (thrust)	FMEP (anti-thrust)	FMEP from asperity (thrust)	FMEP from asperity (anti-thrust)
Cycle 1 (0-720 CAD)	1.854199e-001	1.258643e-001	5.955569e-002	5.938762e-002	1.349374e-004
Cycle 2 (721-1440 CAD)	2.208365e-001	1.635669e-001	5.726954e-002	1.109999e-001	0.000000e+000

VCC	FMEP (i^{th} cycle)	FMEP (thrust)	FMEP (anti-thrust)	FMEP from asperity (thrust)	FMEP from asperity (anti-thrust)
Cycle 1 (0-720 CAD)	2.673459e-001	1.938496e-001	7.349633e-002	1.245211e-001	2.281095e-002
Cycle 2 (721-1440 CAD)	2.643063e-001	1.944686e-001	6.983772e-002	1.297459e-001	2.111408e-002

The total mean effective pressure available by burning the fuel is called the Indicated Mean Effective Pressure. The useful work available from the engine is the Brake Mean Effective Pressure. The difference between the two is the Friction Mean Effective Pressure. It is the effective pressure required to overcome the friction in the engine.

The challenge for the automotive industries is to make the FMEP values as low as possible. Improving this value depends on the skirt design, oil film thickness, expansion due to heat, as well as the friction of the mating surfaces like the piston skirt material and the bore.

In order to show the effects of changing the various input parameters on the FMEP values, a number of simulations have been run. Different cases like changing the viscosity of oil, different engine speeds and different combustion pressure, different oil film thickness etc. have been simulated using the tool to understand how the output parameters described above change with the change in one or two input parameters.

3.2. Simulation Case 1: Low engine speed and low combustion pressure

After the initial case had been run to get the results within the acceptable limits, the tool was used to run a case with lower engine speed and lower combustion pressure. The engine speed defined in the input model file was kept at 1500 rpm instead of 5500 rpm. The pressure file which defines the combustion pressure at every crank angle over a cycle was also changed from MIT which has a peak pressure of 114 bars to VCC which has a peak pressure of 14 bars. This setup gave interesting results most of which were on expected lines.

The peak values of the lateral motion (red) are less than those for the base reference case (blue). The deformations are the same for both the cases so the main difference is the peak combustion pressure force which is much lesser in this case compared to the base case. However, as the lateral motion depends mostly on the clearance which is defined in the input files, the difference is not very large.

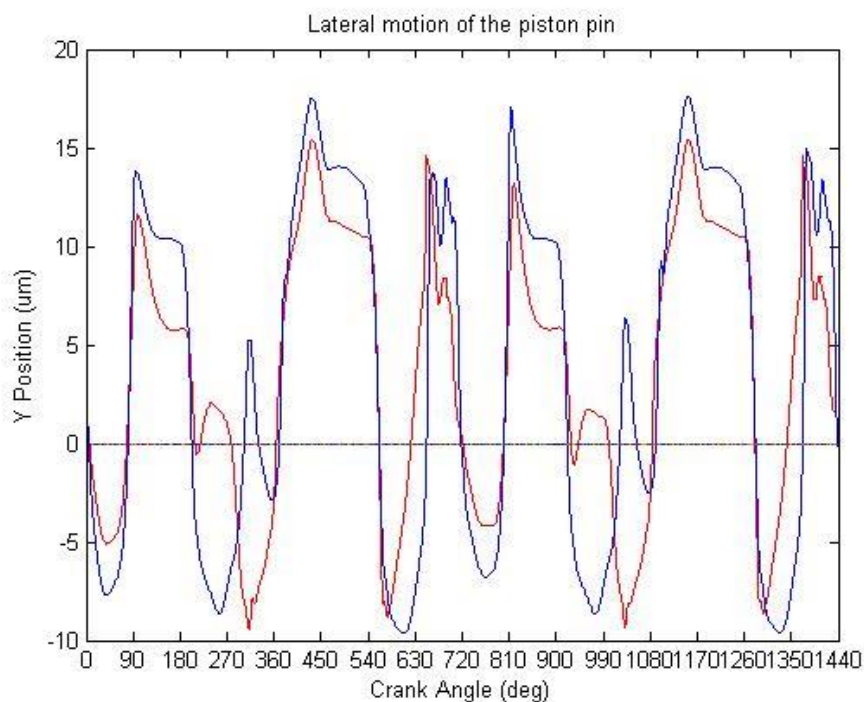


Figure 14: Lateral motion comparison of low engine speed and low peak pressure vs. base reference case

The tilting angle depends more on the pin offset and clearance than the engine speed and the combustion pressure. In the plot above, similar to the lateral motion, it can be seen that the peak values are slightly less but not significant changes compared to the base reference case.

The tilting angle depends more on the pin offset and clearance than the engine speed and the combustion pressure. In the plot above, similar to the lateral motion, it can be seen that the peak values are slightly less but not significant changes compared to the base reference case.

The tilting angle depends more on the pin offset and clearance than the engine speed and the combustion pressure. In figure 15, similar to the lateral motion, it can be seen that the peak values are slightly less but not significant changes compared to the base reference case.

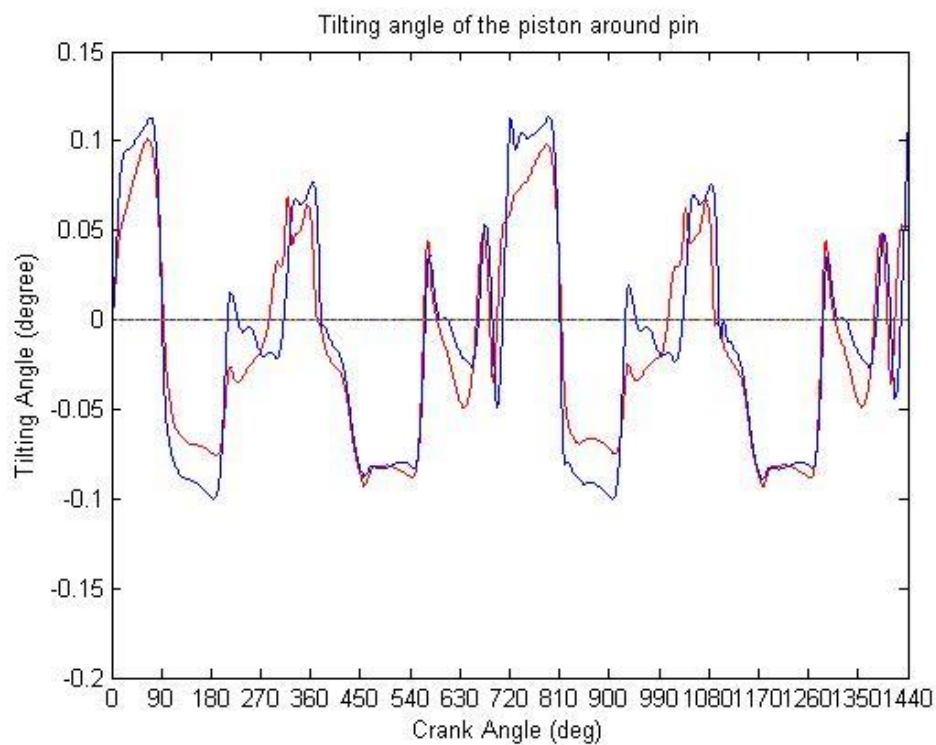


Figure 15: Tilting angle comparison of low engine speed and low peak pressure vs. base reference case

The main parameters that the engine speed and the pressure influence are the forces within the piston including the frictional forces. This is evident in figures 16 and 17.

The side force as seen above is one-sixth of the original value. The curve trend looks smooth however that is because of the scale and the original curve trend for the new case is similar to the reference case. This plot was important as a proof that with the same deformations in both cases, the tool gives results on expected lines. Lower engine speed and lower combustion pressure has to give lesser peak normal forces.

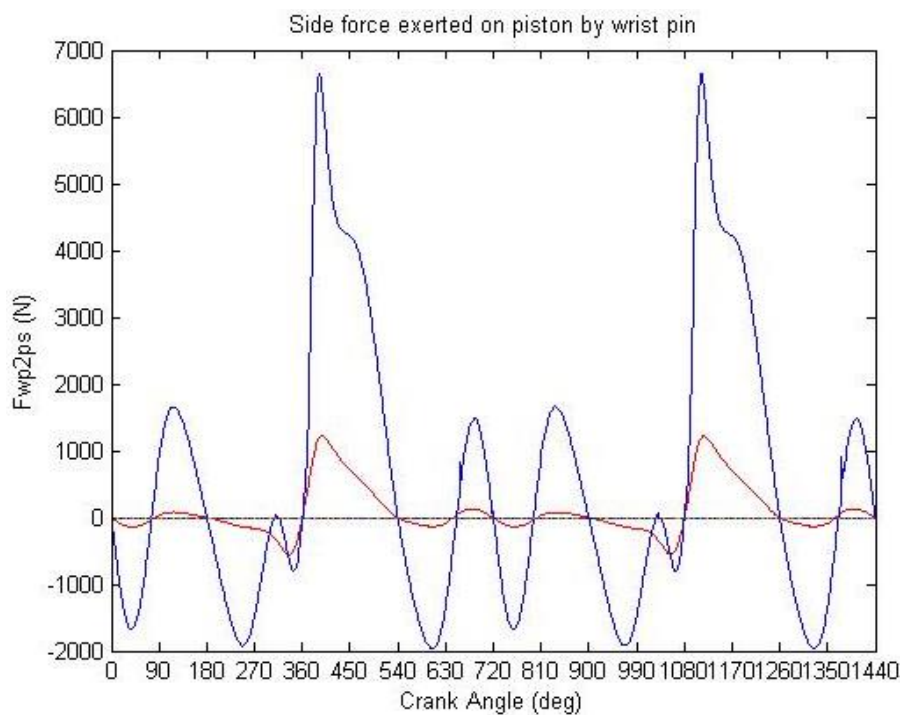


Figure 16: Comparison of side forces between low engine speed and low pressure and the base reference case

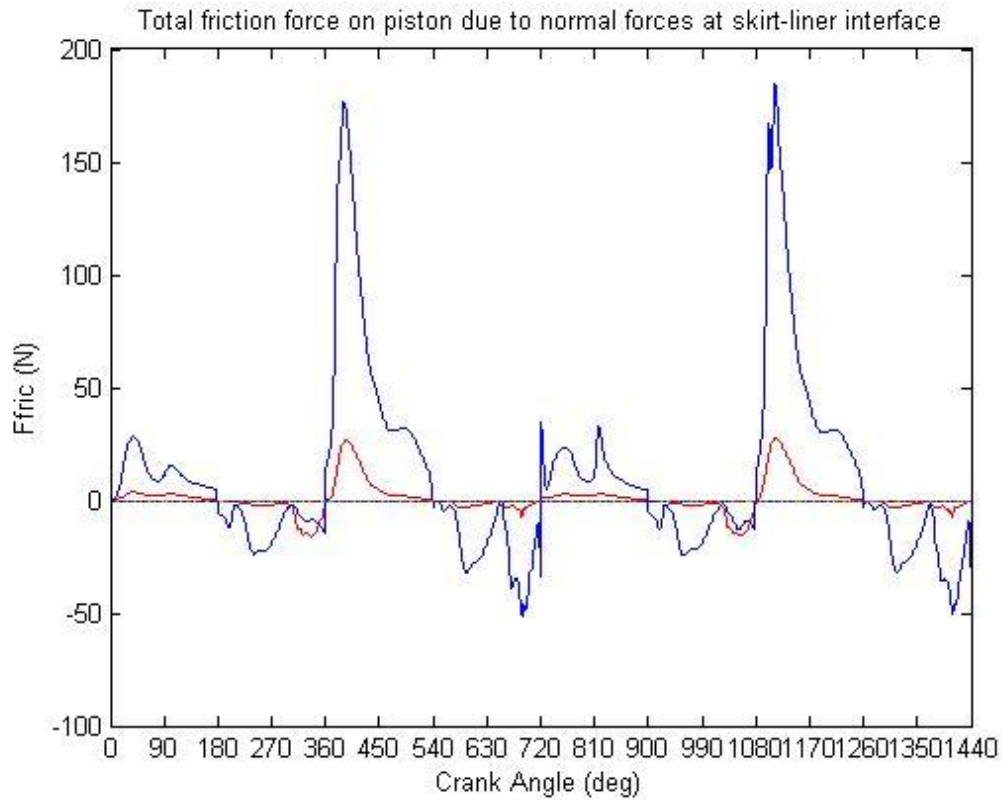


Figure 17: Comparison of friction forces between low engine speed and low pressure and the base reference case

The friction forces, like the side forces above for the new simulation case is one-sixth of the original value with peak at 30 N after ignition. The power loss and the accumulated work loss are also similar which gives the FMEP values approximately one-sixth of the base reference. This comparison of the FMEP values can be better shown in figure 18.

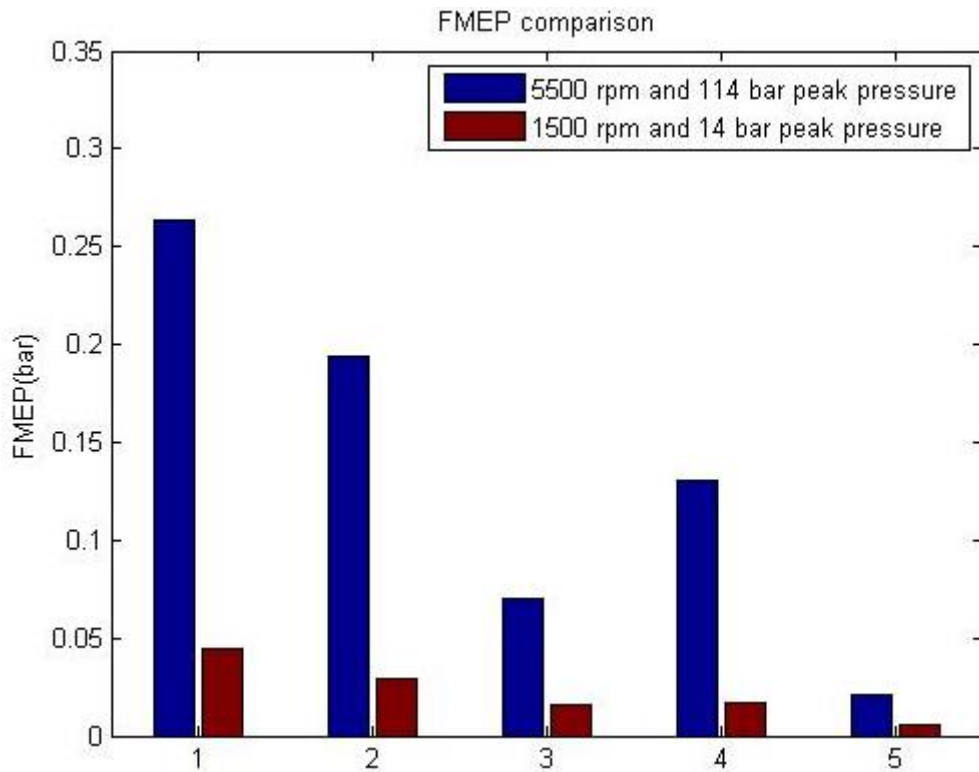


Figure 18: FMEP comparison between case 1 and base reference case

Where the numbers 1-5 on the x-axis indicate

1- FMEP over the whole cycle. This is the FMEP value over 720 crank angle degrees.

2- FMEP (thrust). This is the FMEP value on the thrust side of the piston.

3- FMEP (anti-thrust). This is the FMEP value on the anti-thrust side of the piston.

4- FMEP (thrust due to asperity). This is the FMEP value due to asperity or the surface roughness of the piston on thrust side.

5- FMEP (anti-thrust due to asperity). This is the FMEP value due to asperity or the surface roughness of the piston on anti-thrust side.

3.3. Simulation Case 2: Higher initial oil film thickness

The oil film thickness between the piston and the bore is very important and plays a major role in the friction forces within the piston-cylinder system as has been explained earlier as well in the hydrodynamic forces section. A very small oil film would give rise to lot of scuffing of the piston. The events that lead to this phenomenon are as follows:

- The shortage of oil between the piston ring and the liner causes plastic deformation in surface liners.
- As the clearance between the piston and the liner is in terms of microns, with the absence of oil, the contact area between the piston skirt and the liner increases.
- This leads to metallic contact causing adhesion and leading to wear.

This scuffing is avoided by having oil spray in the piston during the start of every cycle when the piston moves towards the bottom dead position. This oil spray lubricates the contact area between the piston skirt and the cylinder liner preventing metallic contact and thus reducing wear and increasing the life of the engine. Many car manufacturers have an additional oil film supply during the cycle in between to ensure good lubrication. However, in this study, only initial oil film thickness between different parts of the piston like the piston lands, piston chamfer and the piston skirt and the cylinder liner are defined in the input model text file. The program does have the ability to deal with additional oil film supply as well however it requires a special input file to be defined for the same.

The initial oil film thickness for this simulation case was increased from 15 micrometre to 35 micrometres. The simulation gave interesting results. The output values for all the outputs did not change significantly especially the side force and friction force was almost the same. The peak friction force was less by only 6 N compared to the base reference case. The tilting angle in the beginning of the cycle was bit smoother compared to the base case. This can be seen in the plot below.

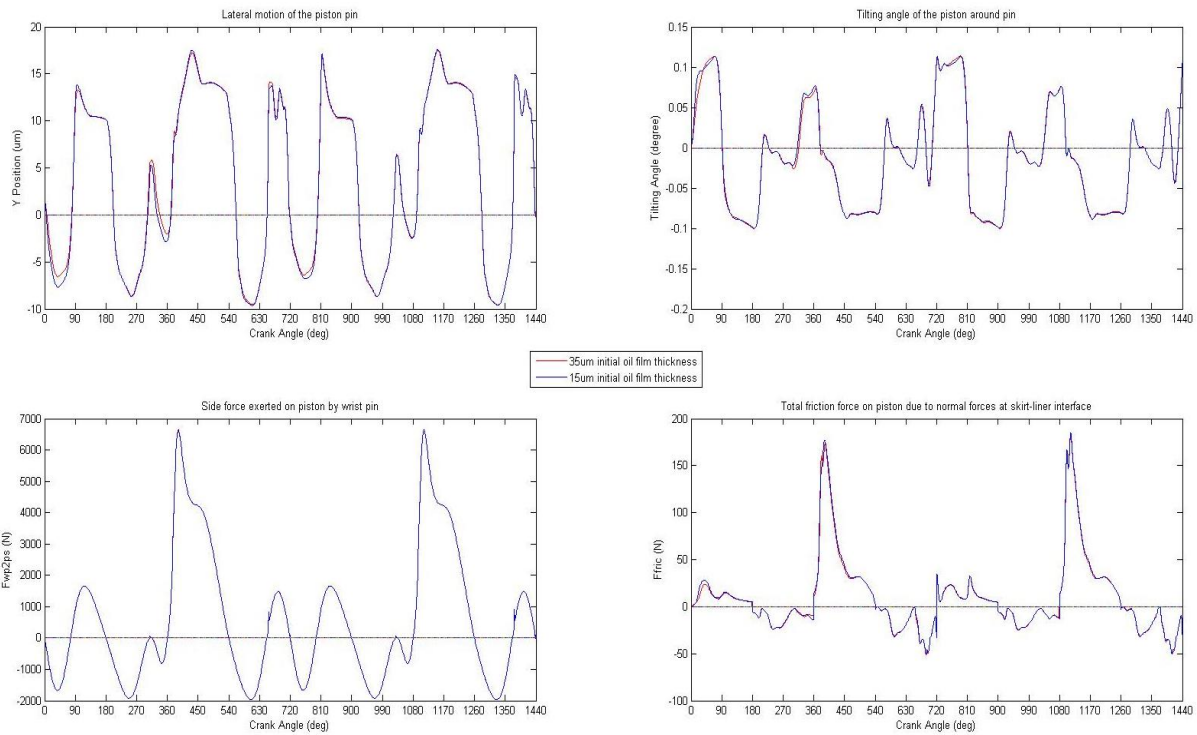


Figure 19: Comparison of results for the base case and higher oil film thickness

The hydrodynamic forces increased by 60 N on both the thrust and the anti-thrust side. This is to be expected as more oil would lead to higher hydrodynamic forces. As seen above, the changes from the base case are only in the initial 90 crank angle degrees after which it almost follows the reference curve. The inference that can be drawn from this is that the initial oil film thickness does not play a major role in the friction forces as the oil will move with the motion of the piston. This is more evident in the FMEP comparison as shown in figure 20.

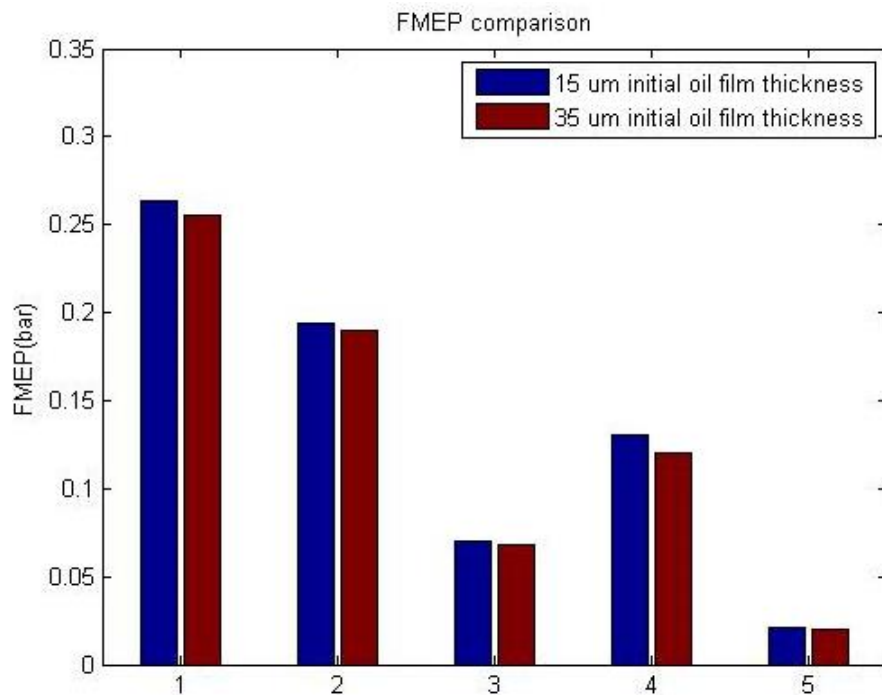


Figure 20: FMEP comparison between case 2 and base reference case

The FMEP values as seen decreases very less for the one with higher initial oil film thickness compared to the base reference case. The difference in the peak values over the whole cycle is less than one-hundredth. Of the different FMEP values, the 4th one which is the FMEP due to asperity on the thrust side of the piston shows more change compared to the other graphs. This is also proof that the tool works well as more oil film thickness leads to lesser surface roughness especially on the thrust side as the thrust side is in contact with the liner after the ignition.

3.4. Simulation Case 3: Larger cold clearance

The cold clearance is defined as the clearance available between the cold piston and the cold bore which means that the thermal expansions are not considered. There has to be some clearance between the piston and the bore to account for the thermal expansions as well as oil film to lubricate the area between the two. This is also important to prevent the wear of the piston and the liner material as insufficient clearance will lead to increased wear. On the other hand, clearance more than the optimal value will lead to vibration of the piston within the cylinder and could lead to more friction.

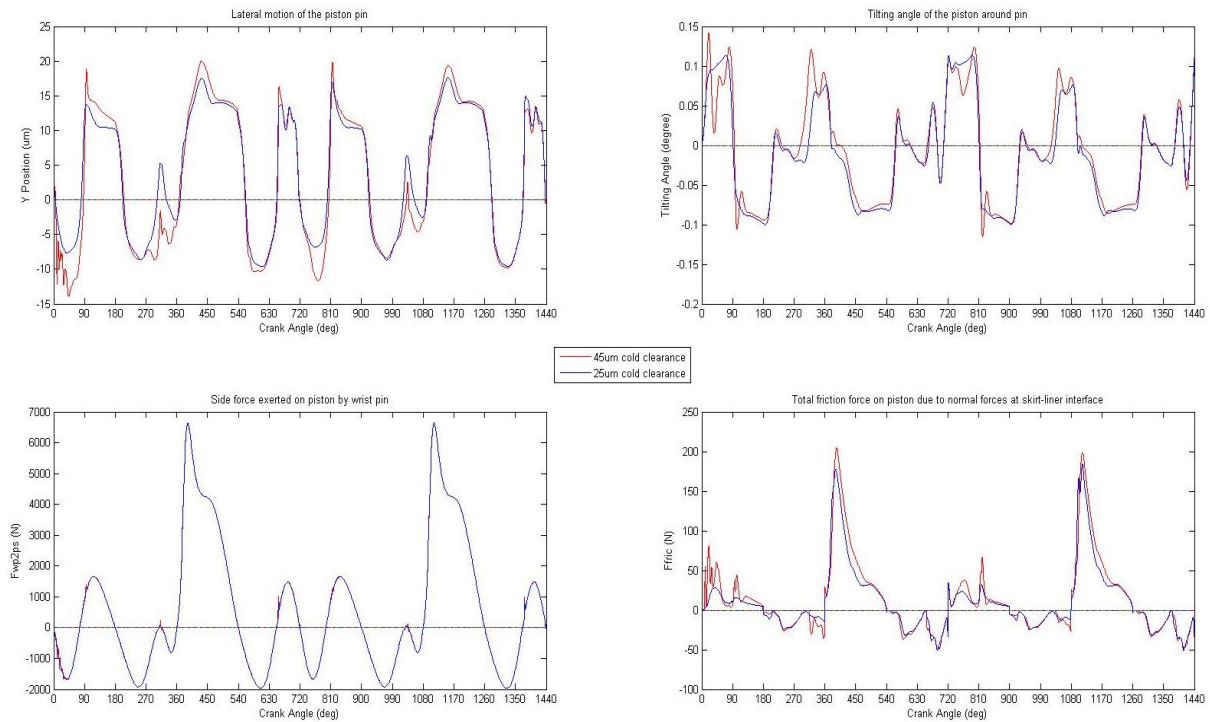


Figure 19: Comparison of results for the base case and higher cold clearance

To understand how the tool responds to the change in the cold clearance, for the third simulation case, the cold clearance between the piston skirt diameter and the cold bore was increased from 25 micrometre to 45 micrometre. The results on the output plots are as shown in figure 21.

The lateral motion and the tilting angle as mentioned earlier depend mostly on the available clearance between the piston skirt and the bore. So increasing the clearance by 20 micrometre increases the peak lateral motion values and tilting angle as seen in figure 21. The side forces are almost the same but the friction forces increase slightly from 180 to 201 N. It is interesting to note the curve trend between 0 to 90 crank angle degrees in all the plots above. This is due to the fact that in the first 90 degrees, there is virtually no thermal expansion and this leads to piston vibration within the cylinder. However, in later part of the cycle, the piston and bore expand thermally decreasing the overall clearance and thus reducing the piston vibrations.

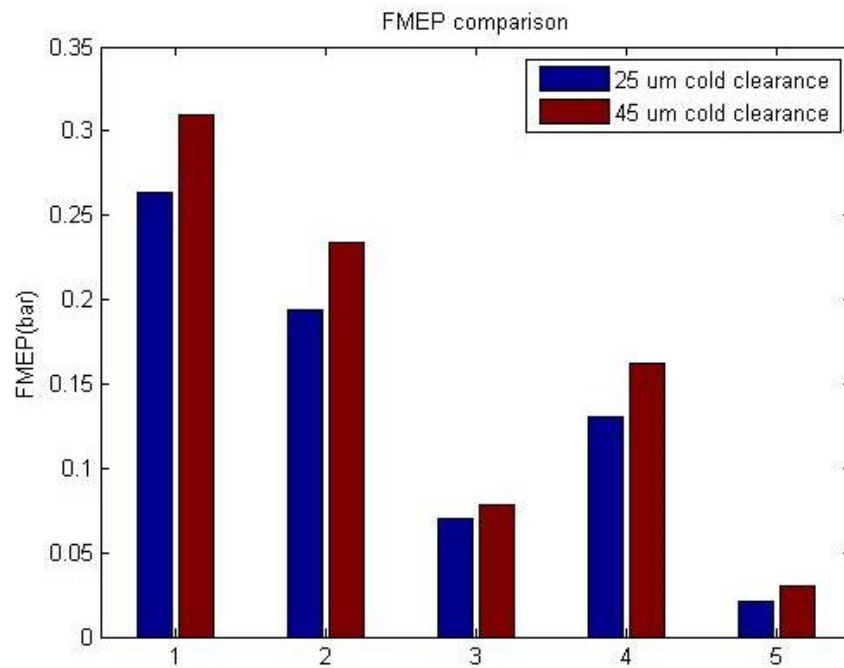


Figure 202: FMEP comparison between case 3 and base reference case

The FMEP values gave an interesting insight into the importance that the clearance plays on the Friction mean pressure. There is a significant increase in the overall FMEP as well as the thrust and anti-thrust FMEP values for the cold clearance case compared to the base reference case. This is because of the fact that higher cold clearance gives rise to more lateral motion which means the piston is hitting the cylinder harder leading to more friction force, more power loss and hence higher FMEP values.

4. Conclusion

The working of the tool is on the basis that has been summarised in the methodology of this report and the detailed explanation in Dongfang Bai's [1] research. The lubrication between the piston skirt and the cylinder affects different properties like friction, wear rate due to scuffing and oil consumption during the piston motion. The solution for the tool is divided in two main parts. One part deals with full flow attachment and applies the Universal Reynolds' equation to calculate the output parameters while the other part deals with the separation model and applies the relevant differential equations for obtaining the solution. The coarse and the fine grids defined for the tool is where the tool is actually working. The coarse grids solutions include the solutions for the normal and the frictional forces which are then interpolated to the fine grids. The fine grids contain the calculation for the lubrication, pressure distribution, shear stress and the oil distribution. This differentiation helps in the results being accurate as well as the simulation time being reasonable.

The friction force and the FMEP values by the tool are within the actual range which not only shows the tool to be working as it should but also that with the limited inputs available, the results from the tool are fairly accurate. In the beginning of the thesis it was assumed that the initial oil film thickness plays a very important part in the friction values but the results from this tool proved that the change in the friction values is not very significant.

The parametric study of the tool was done mainly for the pressure and the engine speed as the temperature files were unavailable. The tool worked well for this case as well. With the same deformation values, the friction and the FMEP values is significantly less for the case with lower pressure and lower engine speed.

The above three simulation cases give us not just a better understanding of the impact of changing the inputs on the output results, but also prove the effectiveness of the P2M tool. It proves that the tool works on expected lines and can be used for a wider range of changes in inputs and help in improving the overall friction which will ultimately help in reducing fuel consumption of the vehicle.

The cases that were run were very basic and the tool has much bigger range of use. The outputs mentioned in this report are not the only outputs given by the tool. It gives many other outputs which include deformation of the nodes at every crank angle for the cylinder and the bore as well as the oil film thickness at every point and at every crank angle degree. However, due to time restrictions that is not included in this report and could be carried over as future work for Volvo Cars.

It is also important to understand that the P2M tool is still in the development phase and Volvo is one of the customers from MIT using this tool. There are few errors in the tool and that has been

communicated to the MIT. There have been some errors in the input files from Volvo as well and so the results are not hundred percent accurate. Few examples include the deformations for the bore that have been considered from the MIT bore but the cylinder length has been fixed to imitate the VCC bore. Also, the chamfer used for the tool is the one from MIT as the VCC one could not be used in its format. All these changes have been modified to be used with the VCC piston so as to have minimum deviations from the actual results. The results have also been compared with the results from the suppliers for the piston and the FMEP values are approximately same as the ones received from the suppliers.

The main conclusion from using this tool is that the outputs depend wholly on the inputs. There are almost 14 input files which need to be defined for the basic case to run. This includes piston and bore cold profiles and the profiles with thermal expansion, deformations due to pressure and inertia, combustion pressure curve among others. The appendix contains information as to how the inputs should be defined for the tool to work without any errors.

It is also important to understand the importance of defining the boundary for the tool to work. In the simulations for the Volvo piston, only the skirt area was defined as the boundary and all the results are for that defined area. The boundary limits are given in the input model file and the rings also can be considered. Furthermore, the clearance between the piston and the bore plays a significant role. Too little will lead to scuffing and wear and too high will lead to more lateral motion, more vibrations and thus more friction and FMEP values.

The tool has certain limitations in the current form. The major limitation lies in the way to treat the oil flow in the skirt area (between skirt and liner). When dealing with partially flooded region (where cavitations occur), the model use a criterion to determine whether to treat the oil film as full attachment or clear separation. For example, if the oil occupancy (oil film thickness/clearance) is larger than 0.6, it is assumed that it attaches both skirt and liner; when it's less than 0.6, the tool assumes that half of the oil film is attached to the liner and the other half to the skirt (and there is void space in the middle). This assumption may result in some discontinuity.

The other limitation is that the cases where the surface of the skirt is worn are not yet considered in the calculation. The assumption in the current model is that there is a uniform waviness on the skirt, which is only accurate when the piston is new.

Finally, the main objective of the thesis was to run the tool for the Volvo piston. The tool is not very user friendly and it took some time to understand the intricacies of its working. However, once it was understood, the simulations run by changing the inputs gave promising results. This tool is in early stages of development and has given close to accurate results. The future of this tool looks good and it is one of the most accurate tools to calculate the secondary motion of the piston.

5. Future Scope

As mentioned above, the tool has wider range of usability than the ones that have been explored as part of this thesis work. The tool has the ability to compute many different complex phenomena occurring in the piston-cylinder system. Some of the additional work which can be carried out with the current work includes the following:

- In the current simulation case, only the compliance of the piston skirt has been taken into consideration. The inverse of the stiffness matrix is the compliance matrix. The tool has the ability to consider the liner compliance as well to give better results. A different input file for the liner compliance needs to be defined for the same.
- The tool also has the ability to consider the effect of viscosity on the oil. For this, the temperature at every crank angle degree needs to be defined as another input file. There are some viscosity constants which are defined in the input model file. Using this viscosity feature of the tool will give more realistic results as viscosity of oil is an important phenomenon that occurs within the piston cylinder system.
- The tool can give the results within 12 hours for simulating 2 cycles. This means that different skirt designs can be simulated as well as the different oil flow regulations can be studied. This will lead to faster and more reliable results for the friction and FMEP values and improving the overall fuel efficiency of the engine.
- A script for visualizing the motion of the piston within the cylinder bore and the distribution of the oil film at different stages of the piston motion can be written for better understanding of this complex phenomenon.

This thesis has been important from the point of view that with increasing legislations on pollution from automobiles and fuel consumption issues, the research in the field of friction has grown intensely in the last decade. Also, necessary to understand is that the simulation and analysis takes more importance than actual testing as it is more economical, gives better results and can be repeated with small changes to give different results as well. All this is why the P2M tool by MIT has been used by a consortium of different OEM's and suppliers including Volvo Car Corporation for studying the secondary motion of the piston. There is a lot of research work still pending in this field and the tool too has a long way to go in being more user friendly and computing more realistic scenarios to give accurate results.

References

- [1] Dongfang Bai, Modelling Piston Skirt Lubrication in Internal Combustion Engines, Massachusetts Institute of Technology, 2012, citable URI: <http://hdl.handle.net/1721.1/74901>.
- [2] Federal-Mogul Burscheid GmbH, Piston Ring Handbook, August 2008.
- [3] <http://www.serviscreen.com/serviscreengallery/index.php>, accessed on 24 April 2016.
- [4] M.F. Ahmad Fakaruddin, A. Mohd Hafiz and K.Karmegam, Materials selection for wet cylinder liner, IOSR Journal of Engineering (IOSRJEN) e-ISSN: 2250-3021, September 2012.
- [5] <https://www.highpowermedia.com/blog/3126/piston-skirt-coatings>, accessed on 15 April 2016.
- [6] Tian Tian, Modelling the performance of the piston ring-pack in internal combustion engines, Massachusetts Institute of Technology, 1997, citable URI: <http://hdl.handle.net/1721.1/10445>.
- [7] Benoist Thirouard, Characterization and Modelling of the fundamental aspects of oil transport in the piston ring pack of internal combustion engines, Massachusetts Institute of Technology, 2001, citable URI: <http://hdl.handle.net/1721.1/8890>.
- [8] Camille Baelden, A multi-scale model for piston ring dynamics, lubrication and oil transport in internal combustion engines, 2014, citable URI: <http://hdl.handle.net/1721.1/92151>.
- [9] Conor McNelly, Development of a numerical model of piston secondary motion for internal combustion engines, Massachusetts Institute of Technology, 2000, citable URI: <https://dspace.mit.edu/bitstream/handle/1721.1/26880/46310081-MIT.pdf?sequence=2>.
- [10] Zhen Meng, Input and Output of the Piston Secondary Motion (P2M) Model Version 5, Sloan Automotive Laboratory, Massachusetts Institute of Technology, 2016.
- [11] Pasquale Totaro, Modelling piston secondary motion and skirt lubrication with applications, Massachusetts Institute of Technology, 2014, citable URI: <http://hdl.handle.net/1721.1/92125>.
- [12] Reynolds equation, https://en.wikipedia.org/wiki/Reynolds_equation, accessed on 20 May 2016.